Graphics for core-complex morphology and geologic continuous casting

by Jon E. Spencer
Arizona Geological Survey
Open-File Report 09-03
version 1.0

Some relevant citations:

Spencer, J.E., 1999, Geologic continuous casting below continental and deep-sea detachment faults and at the striated extrusion of Sacsayhuamán, Peru: Geology, v. 27, p. 327-330.

Spencer, J.E., 2000, Possible origin and significance of extension-parallel drainages in Arizona's metamorphic core complexes: Geological Society of America Bulletin, v. 112, p. 727-735.

Spencer, J.E., 2001, Possible giant metamorphic core complex at the center of Artemis Corona, Venus: Geological Society of America Bulletin, v. 113, p. 333-345.

Spencer, J.E., and Ohara, Y., 2008, Magmatic and tectonic continuous casting in the circum-Pacific region, *in* Spencer, J.E., and Titley, S.R., eds., Ores and orogenesis: Circum-Pacific tectonics, geologic evolution, and ore deposits: Arizona Geological Society Digest 22, p. 31-53.

Spencer, J.E., 2009, Graphics for core-complex morphology and geologic continuous casting: Arizona Geological Survey Open-File Report 09-03, PowerPoint file and associated graphics.

The essential process in continuous casting is cooling and solidification of the cast medium during heat loss across a slip surface followed by extrusion from a mold.

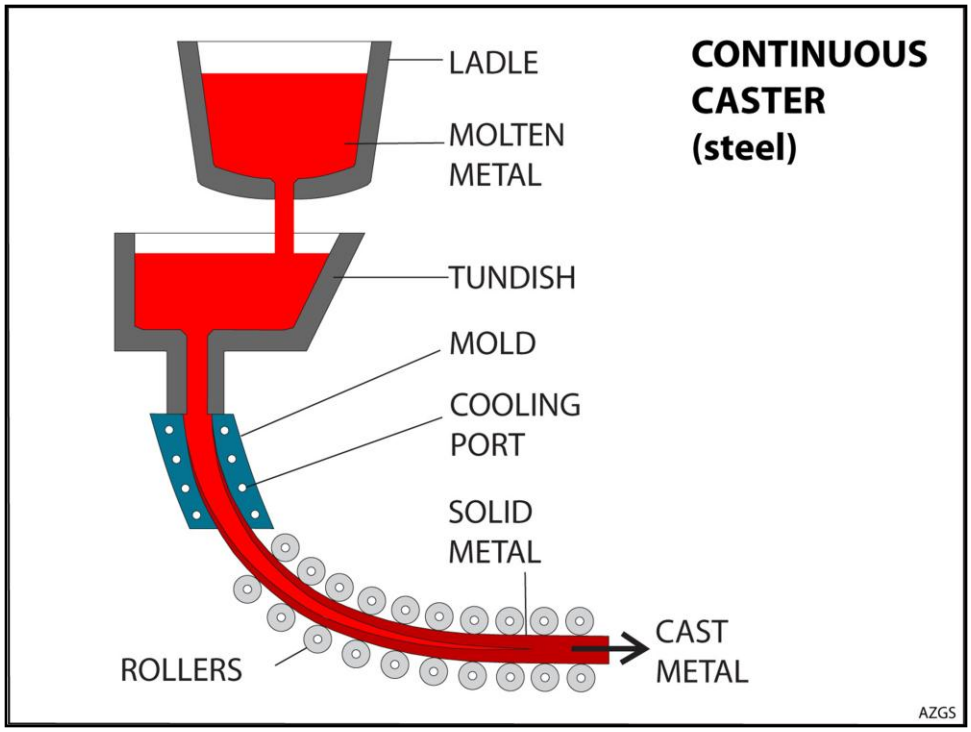
CONTINUOUS CASTER (steel)
LADLE
MOLTEN METAL
TUNDISH
MOLD
COOLING PORT
SOLID METAL
CAST METAL
ROLLERS
AZGS

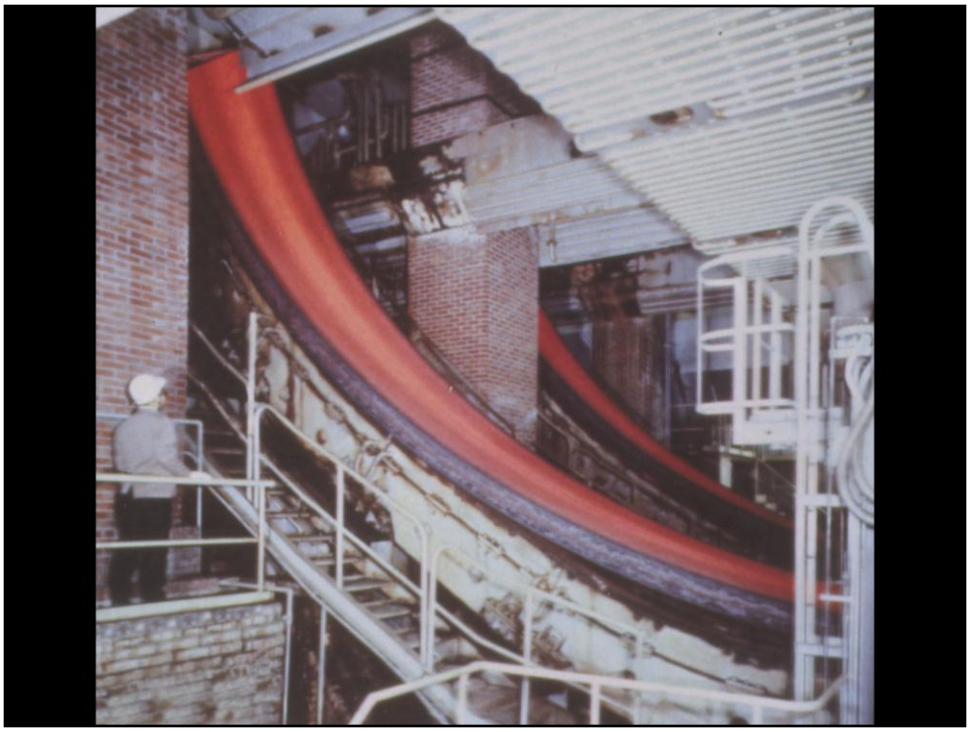

Continuous casting of steel, showing hot steel immediately after extrusion.

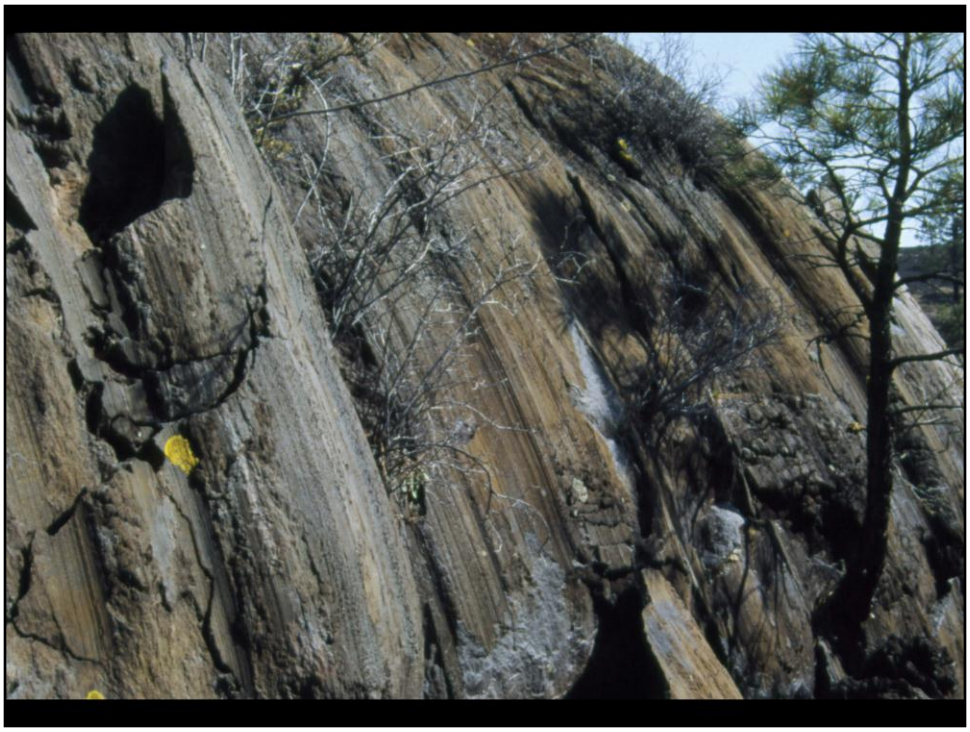

Lava squeeze-up near Sunset Crater northeast of Flagstaff (photo by Jon Spencer)

Striated side of lava squeeze-up near Sunset Crater northeast of Flagstaff (photo by Jon Spencer)

Striated side of lava squeeze-up near Sunset Crater northeast of Flagstaff (photo by Jon Spencer). During extrusion, the exterior of the squeeze up became sufficiently cool and brittle that it cracked and striated fragments separated, mainly along fractures perpendicular to slip direction. However, the interior of the squeeze up remained sufficiently hot and ductile that it did not fracture. One can imagine a paste-like exterior with a hotter and more ductile interior.

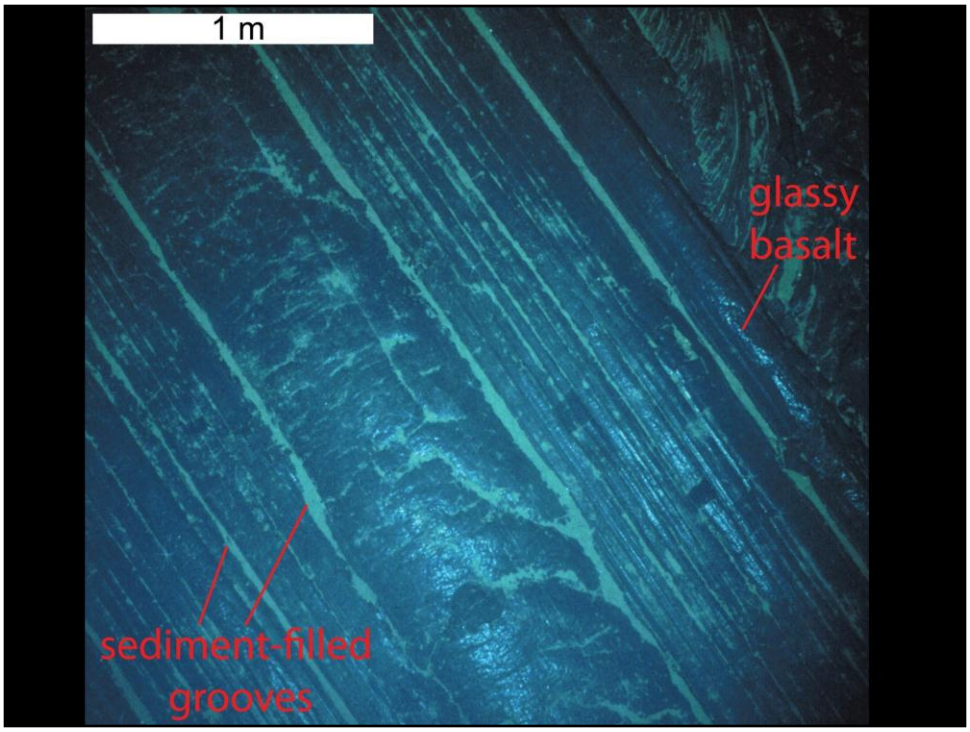

Striated top of a submarine lava flow at the Jaun de Fuca spreading center. Striations are interpreted to have formed during lava flow from beneath the solid crust of a submarine lava lake, with striations produced where molten lava was abruptly chilled by sea water immediately after flow from beneath the irregular underside of the lava-lake crust. Photo provided by Bill Chadwick.

See: Chadwick, W.W., Jr., Gregg, T.K.P., and Embley, R.W., 1999, Submarine lineated sheet flows: a unique lava morphology formed on subsiding lava ponds: Bulletin of Volcanology, v. 61, p. 194-206.

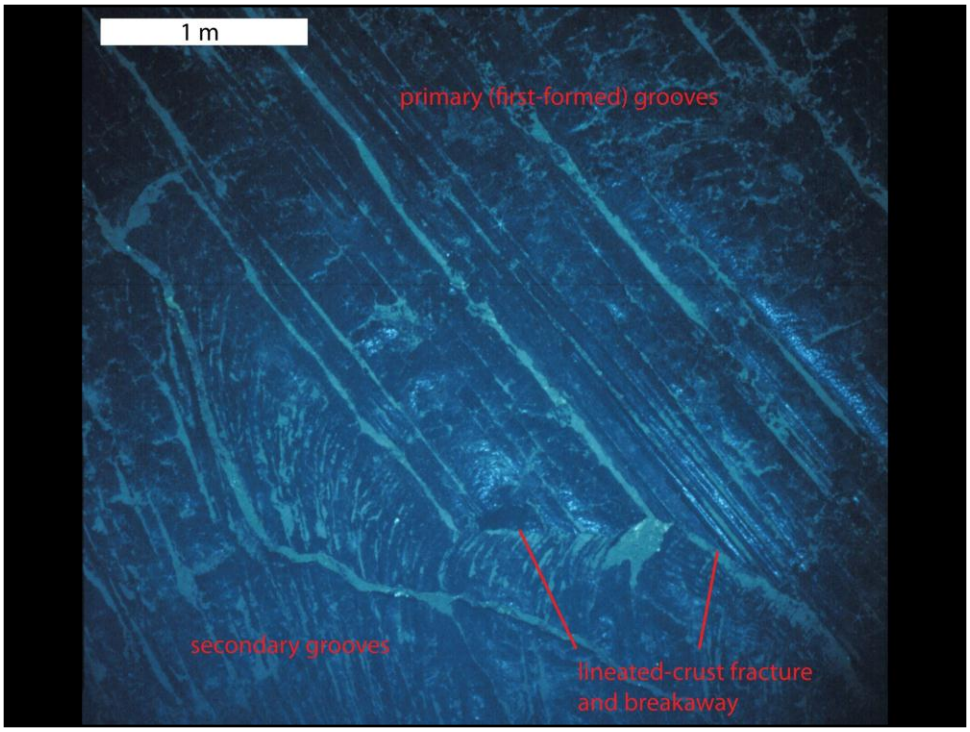

Striated top of a submarine lava flow at the Jaun de Fuca spreading center. Striations are interpreted to have formed during lava flow from beneath the solid crust of a submarine lava lake, with striations produced where molten lava was abruptly chilled by sea water immediately after flow from beneath the irregular underside of the lava-lake crust. Photo provided by Bill Chadwick.

See: Chadwick, W.W., Jr., Gregg, T.K.P., and Embley, R.W., 1999, Submarine lineated sheet flows: a unique lava morphology formed on subsiding lava ponds: Bulletin of Volcanology, v. 61, p. 194-206.

Striated fine-grained diorite at Sacsayhuaman, Cusco, Peru. Photo by Roland Brady (Cal State Fresno). See Spencer (1999) for discussion of origin by continuous casting and citations within for discussion of diverse other origins. See especially: Feininger, T., 1978, The extraordinary striated outcrop at Saqsaywaman, Peru: Geological Society of America Bulletin, v. 89, p. 494-503.

Striated fine-grained diorite at Sacsayhuaman, Cusco, Peru. Photo by Roland Brady (Cal State Fresno). See Spencer (1999) for discussion of origin by continuous casting and citations within for discussion of diverse other origins. See especially: Feininger, T., 1978, The extraordinary striated outcrop at Saqsaywaman, Peru: Geological Society of America Bulletin, v. 89, p. 494-503.

Striated fine-grained diorite at Sacsayhuaman, Cusco, Peru. Photo by Roland Brady (Cal State Fresno). See Spencer (1999) for discussion of origin by continuous casting and citations within for discussion of diverse other origins. See especially: Feininger, T., 1978, The extraordinary striated outcrop at Saqsaywaman, Peru: Geological Society of America Bulletin, v. 89, p. 494-503.

Striated extrusion within the Mt. Saint Helens crater.
Iverson, R.M., Dzurisin, D., Gardner, C.A., Gerlach, T.M., LaHusen, R.G., Lisowski, M., Major, J.J., Malone, S.D., Messerich, J.A., Moran, S.C., Pallister, J.S., Qamar, A.I., Schilling, S.P., Vallance, J.W., 2006, Dynamics of seismogenic volcanic extrusion at Mount St Helens in 2004–05: Nature, v. 444, p. 439-443; doi:10.1038/nature05322.

Striated extrusion within the Mt. Saint Helens crater.
Iverson, R.M., Dzurisin, D., Gardner, C.A., Gerlach, T.M., LaHusen, R.G., Lisowski, M., Major, J.J., Malone, S.D., Messerich, J.A., Moran, S.C., Pallister, J.S., Qamar, A.I., Schilling, S.P., Vallance, J.W., 2006, Dynamics of seismogenic volcanic extrusion at Mount St Helens in 2004–05: Nature, v. 444, p. 439-443; doi:10.1038/nature05322.

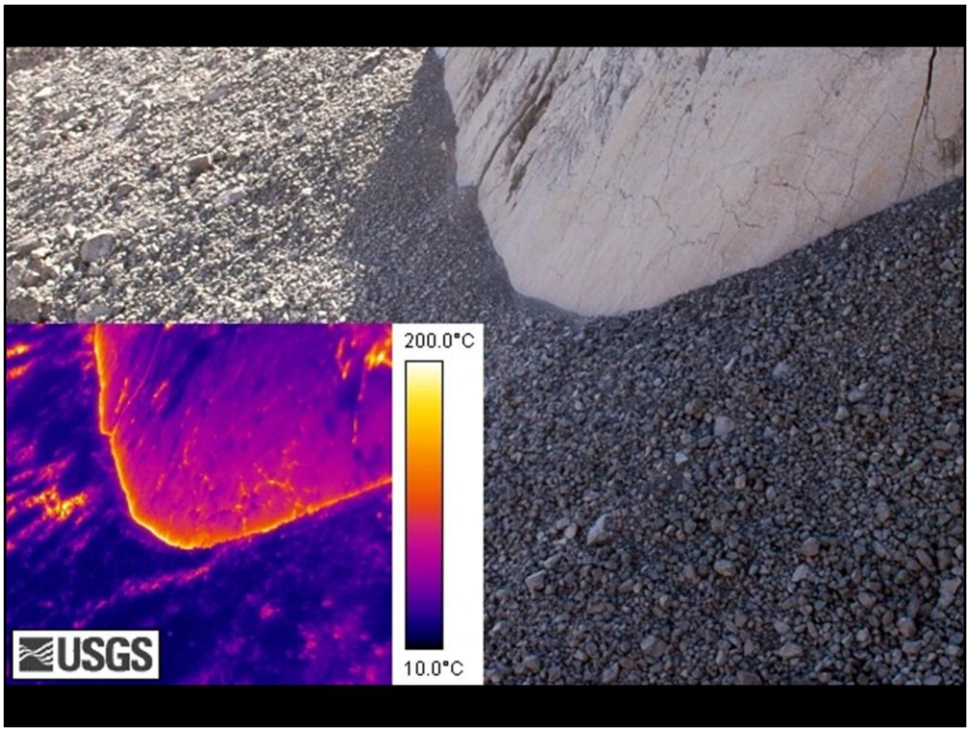

Striated extrusion within the Mt. Saint Helens crater.
Iverson, R.M., Dzurisin, D., Gardner, C.A., Gerlach, T.M., LaHusen, R.G., Lisowski, M., Major, J.J., Malone, S.D., Messerich, J.A., Moran, S.C., Pallister, J.S., Qamar, A.I., Schilling, S.P., Vallance, J.W., 2006, Dynamics of seismogenic volcanic extrusion at Mount St Helens in 2004–05: Nature, v. 444, p. 439-443; doi:10.1038/nature05322.

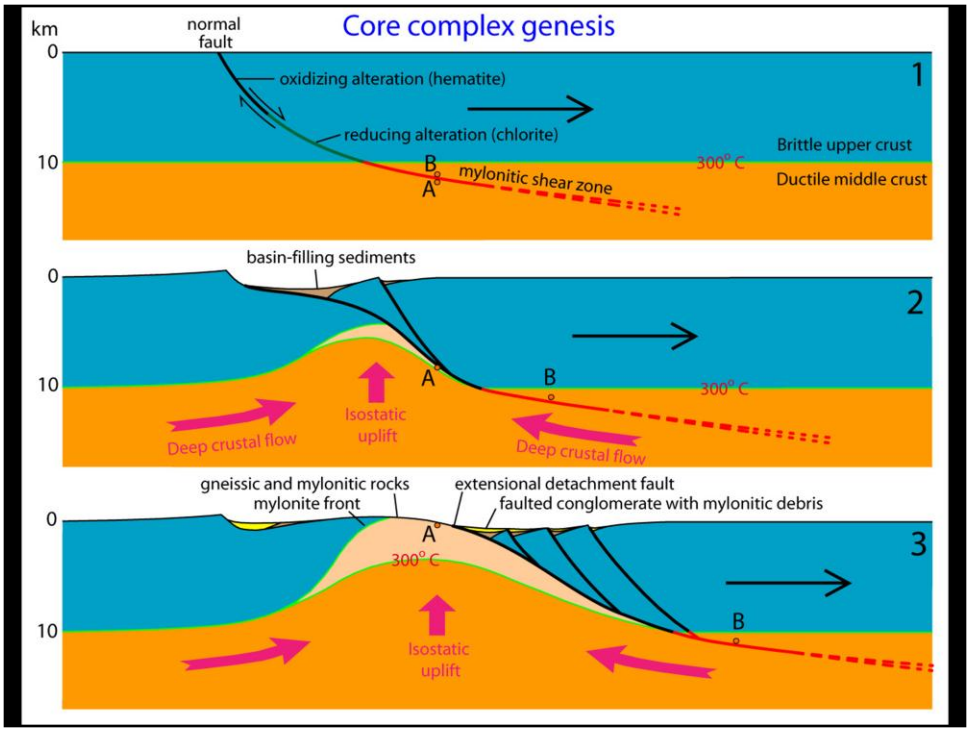

Core complex evolution in cross section. Modified from Spencer and Ohara (2008).

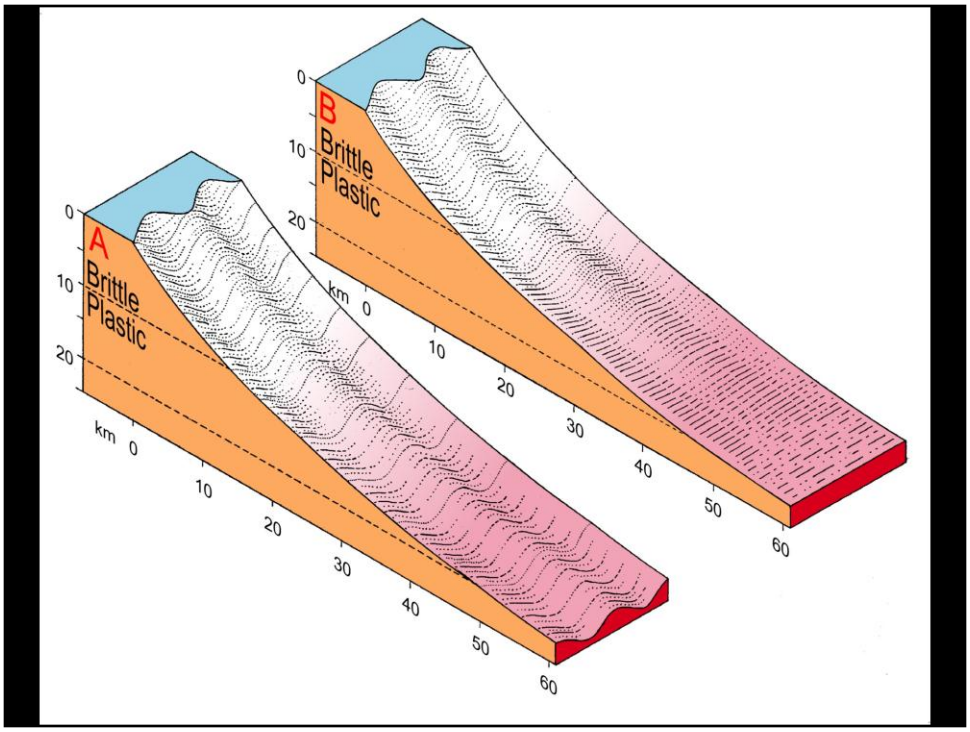

Alternative geometries for core complex footwalls upon initiation of extension. Configuration A results in no footwall molding or shaping during exhumation, but provides no explanation for groove continuity. Slip with configuration B results in molding of deep parts of the footwall to the grooved underside of the colder and stronger hanging wall, followed by exhumation of cast grooves. From Spencer (1999).

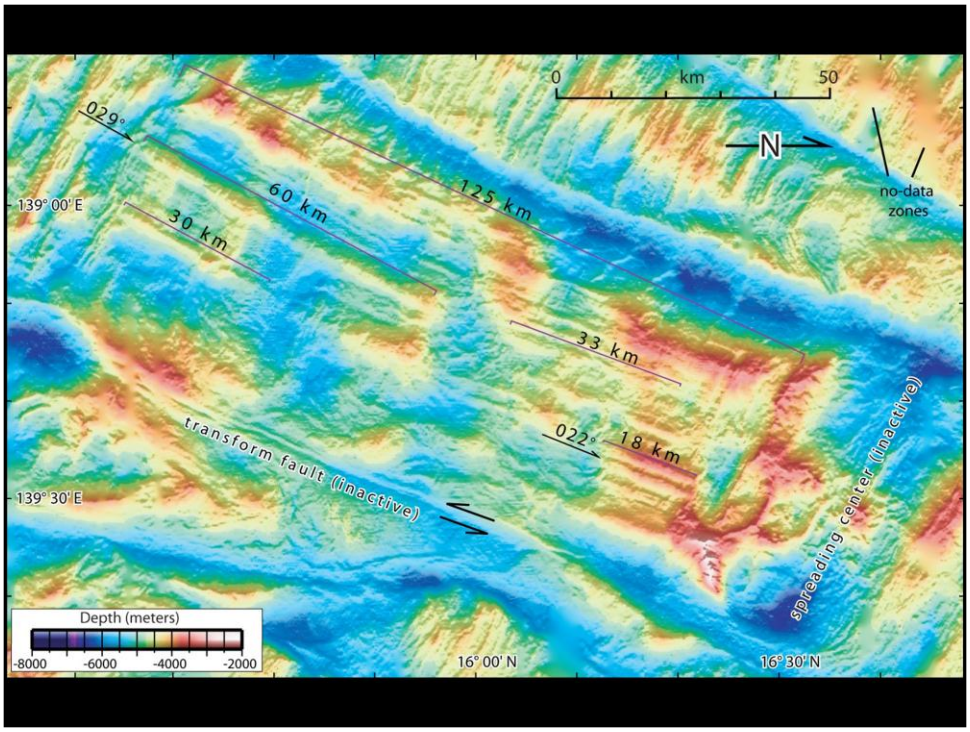

Godzilla mullion in the Philippine Sea. See Ohara, Y., Yoshida, T., Kato, Y., and Kasuga, S., 2001, Giant megamullion in the Parece Vela backarc basin: Marine Geophysical Researches, v. 22, p. 47-61. Modified from Spencer and Ohara (2008). This is the largest grooved core complex known on Earth.

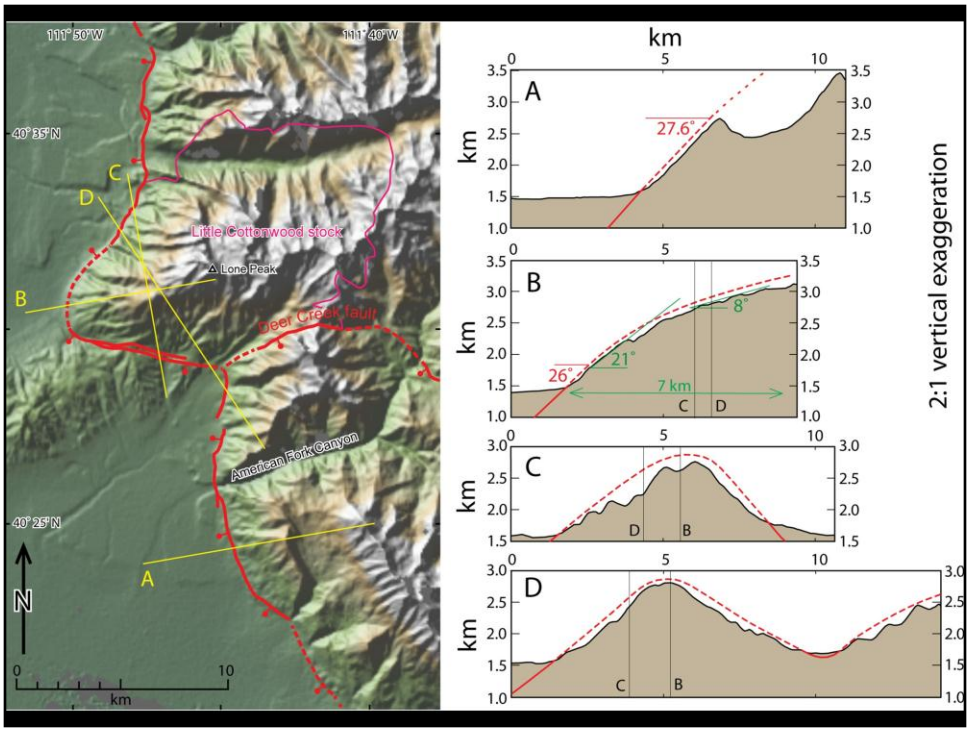

Wasatch Front south of Salt Lake City. Irregular form of normal-fault footwall is apparent. The footwall is not molded, but continued displacement will eventually introduce hot, deep crustal rocks to the colder and stronger grooved underside of the hanging wall block, resulting in corrugation genesis by continuous casting. From Spencer and Ohara (2008). Topography derived from the Shuttle Radar Topography Mission digital elevation model, rendered using GeoMapApp.

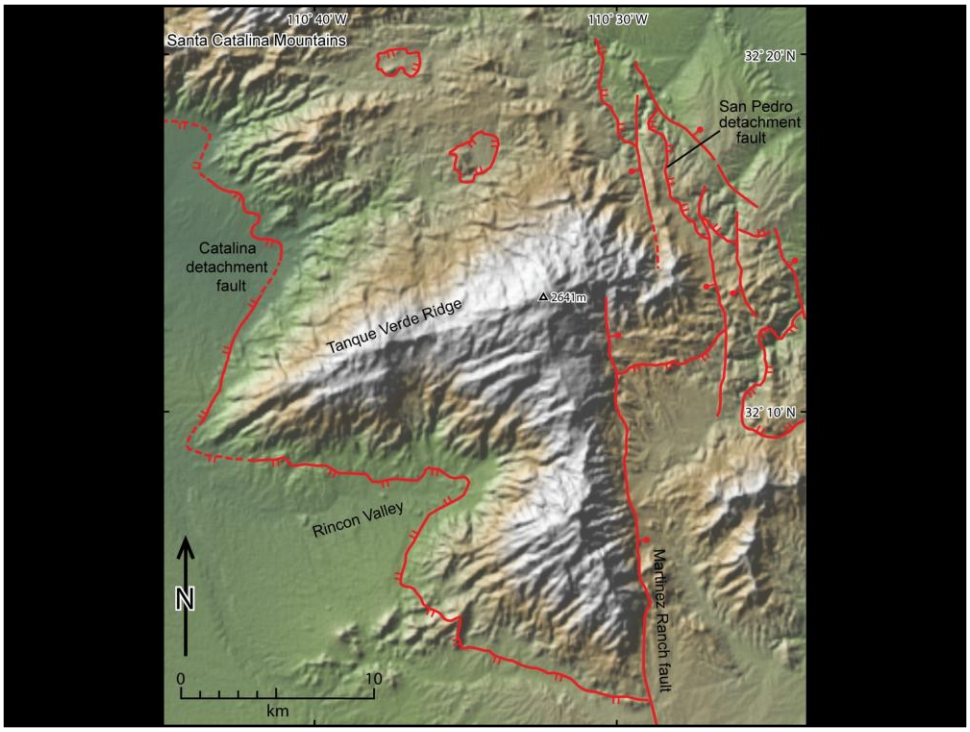

Rincon Mountains east of Tucson, Arizona. Tanque Verde Ridge is one of the largest know core-complex grooves. Note also parallel drainages (see Spencer, 2000). From Spencer and Ohara (2008). Topography derived from the Shuttle Radar Topography Mission digital elevation model, rendered using GeoMapApp.

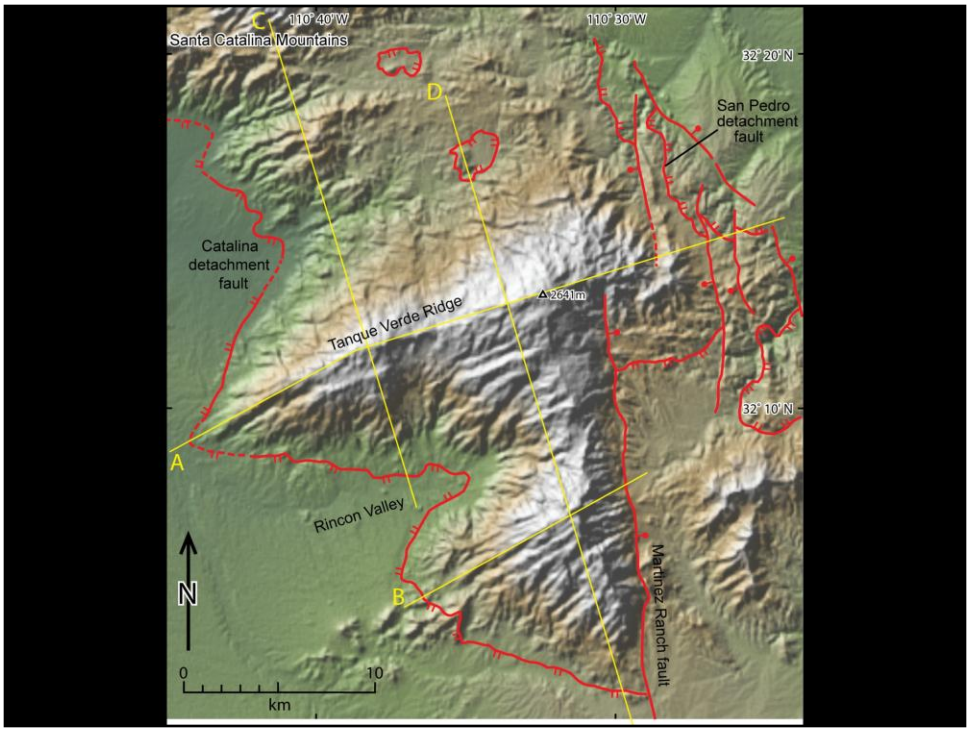

Rincon Mountains east of Tucson, Arizona, with location of cross sections. Tanque Verde Ridge is one of the largest know core-complex grooves. Note also parallel drainages (see Spencer, 2000). From Spencer and Ohara (2008). From Spencer and Ohara (2008). Topography derived from the Shuttle Radar Topography Mission digital elevation model, rendered using GeoMapApp.

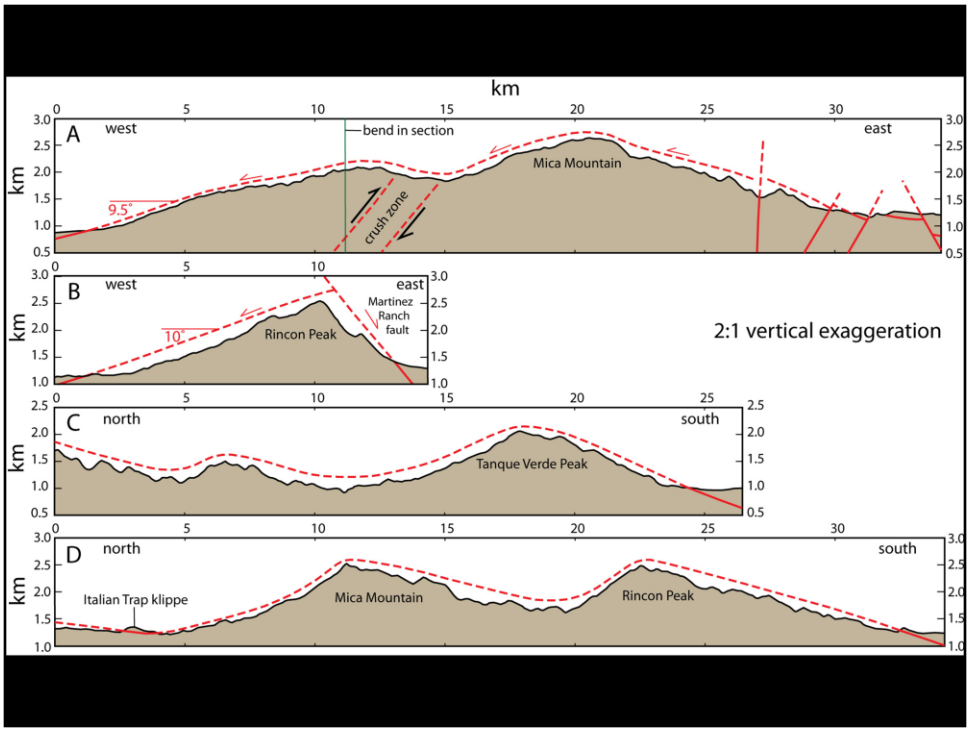

Cross sections through the Rincon Mountains, part of the Catalina metamorphic core complex. From Spencer and Ohara (2008). Topography derived from the Shuttle Radar Topography Mission digital elevation model, rendered using cross section tool in GeoMapApp.

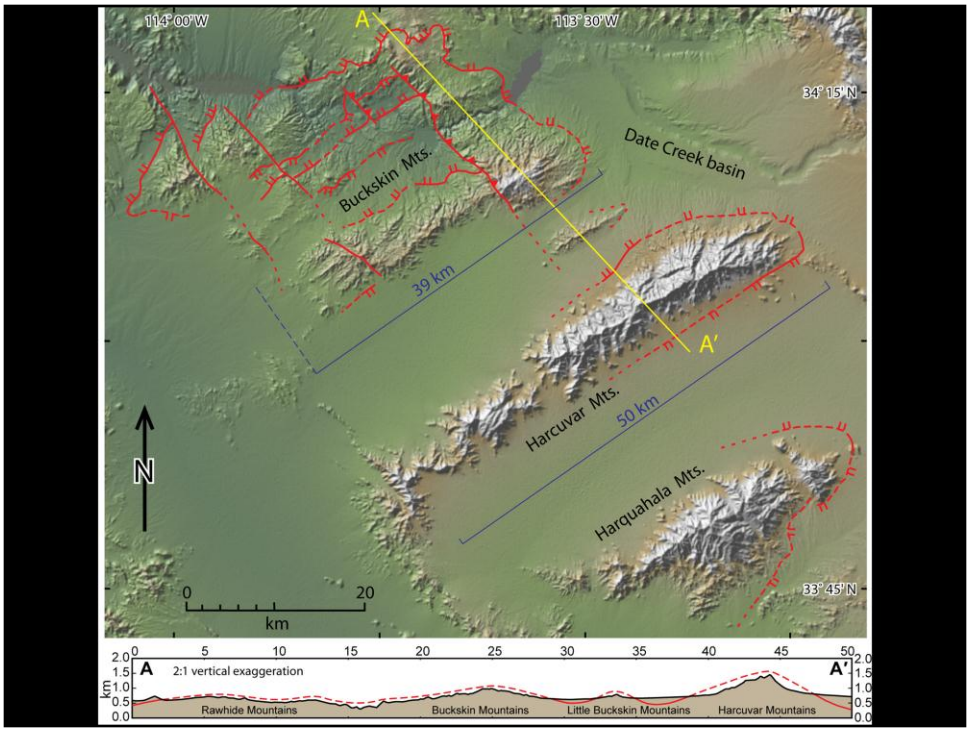

Buckskin-Rawhide-Harcuvar core complex in western Arizona. From Spencer and Ohara (2008). Topography derived from the Shuttle Radar Topography Mission digital elevation model, rendered using GeoMapApp.

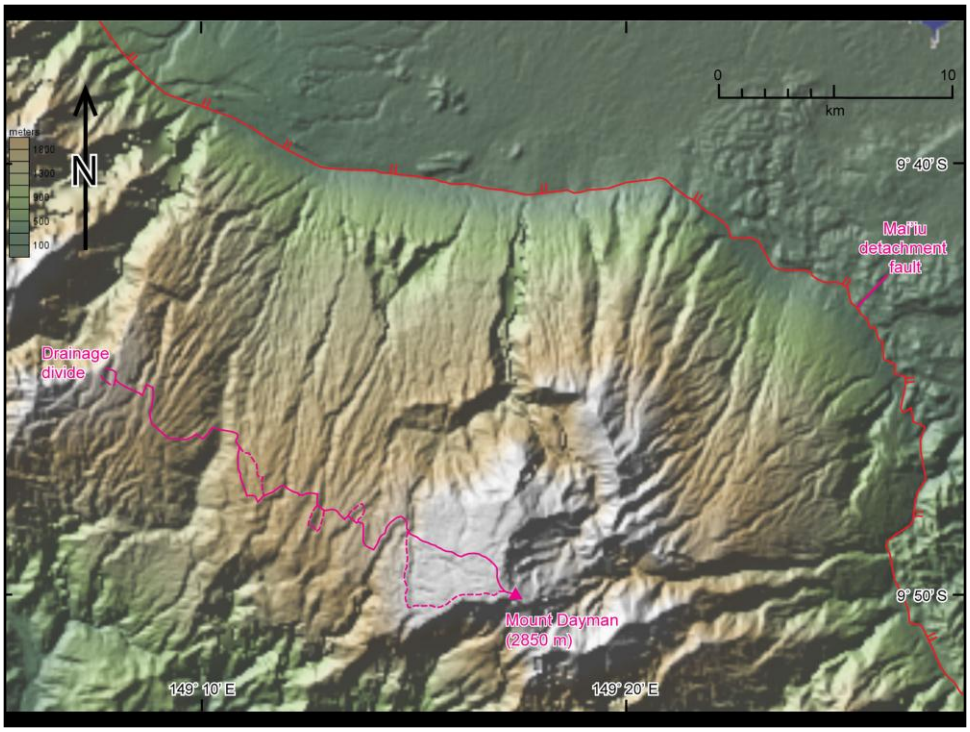

Dayman Dome metamorphic core complex in eastern Papua New Guinea. Modified from Spencer and Ohara (2008). Topography derived from the Shuttle Radar Topography Mission digital elevation model, rendered using GeoMapApp.

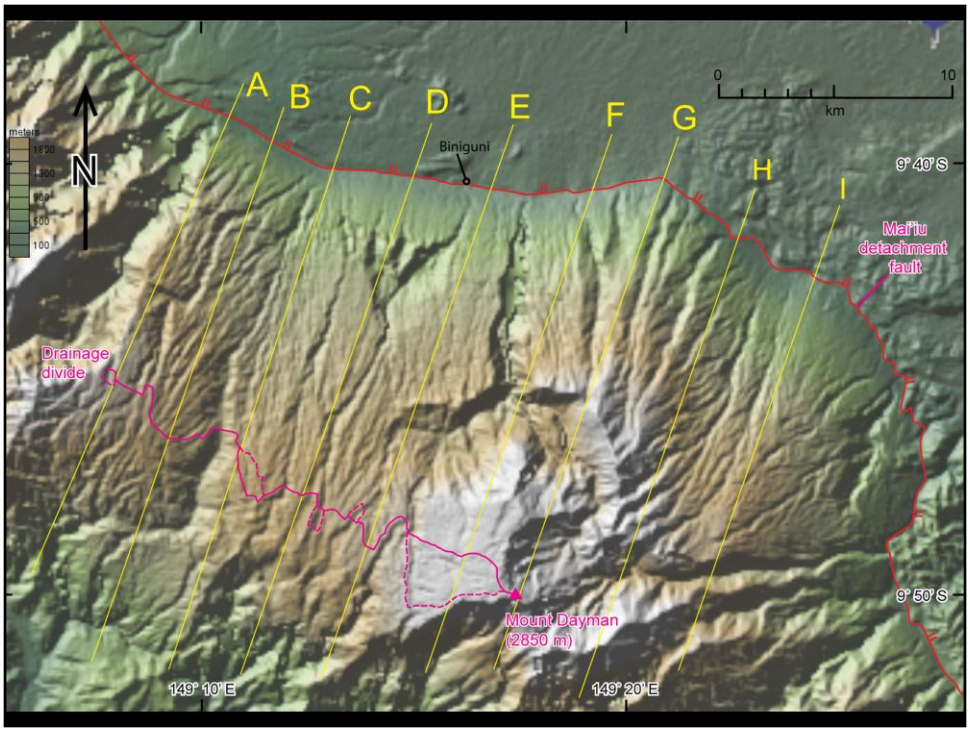

Dayman Dome metamorphic core complex in eastern Papua New Guinea, showing location of cross sections. Modified from Spencer and Ohara (2008).

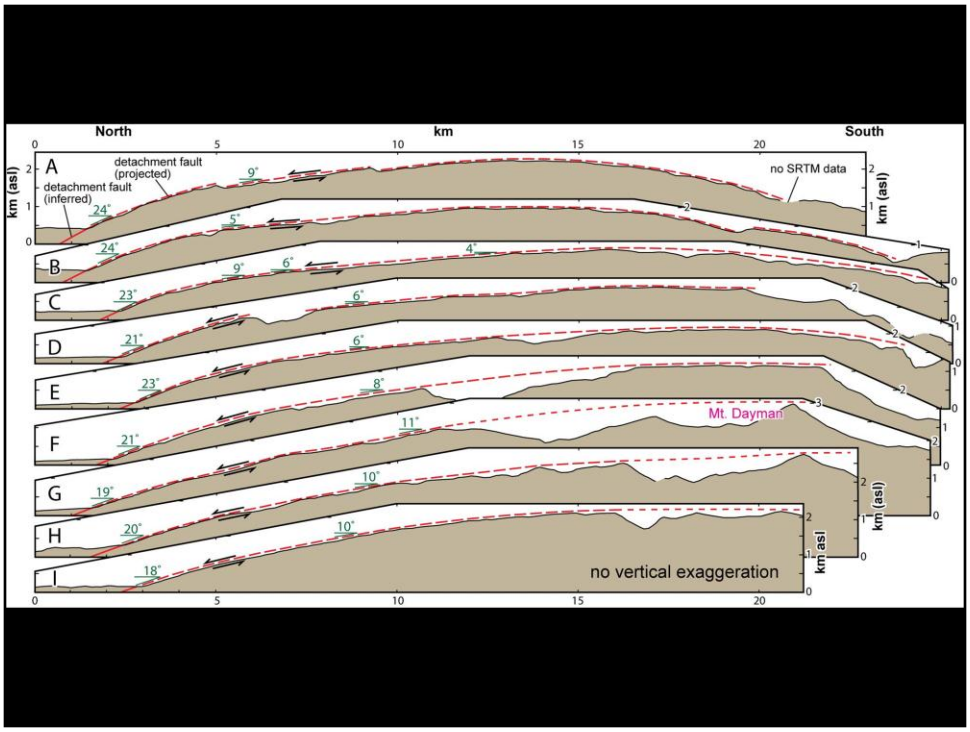

Cross sections of Dayman Dome metamorphic core complex in eastern Papua New Guinea. Modified from Spencer and Ohara (2008). Topography derived from the Shuttle Radar Topography Mission digital elevation model, rendered using cross section tool in GeoMapApp.

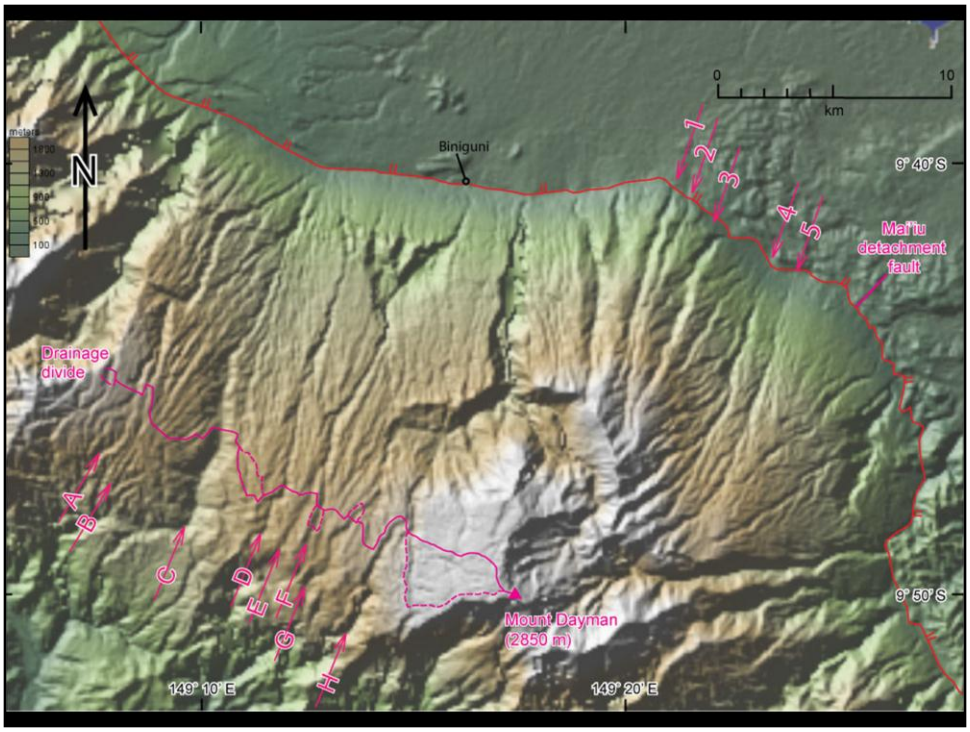

Dayman Dome metamorphic core complex in eastern Papua New Guinea showing locations of aligned drainages. Drainages 1 through 5 are parallel to extension direction and do not plunge directly down slope. Drainages 3 and 4 can be seen to capture drainages that plunge directly down slope, and to divert them into parallelism with extension direction. These are possible candidates for modern, extension parallel drainages with control over drainage geometry exerted by canyons in the hanging wall block (see Spencer, 2000). Modified from Spencer and Ohara (2008).

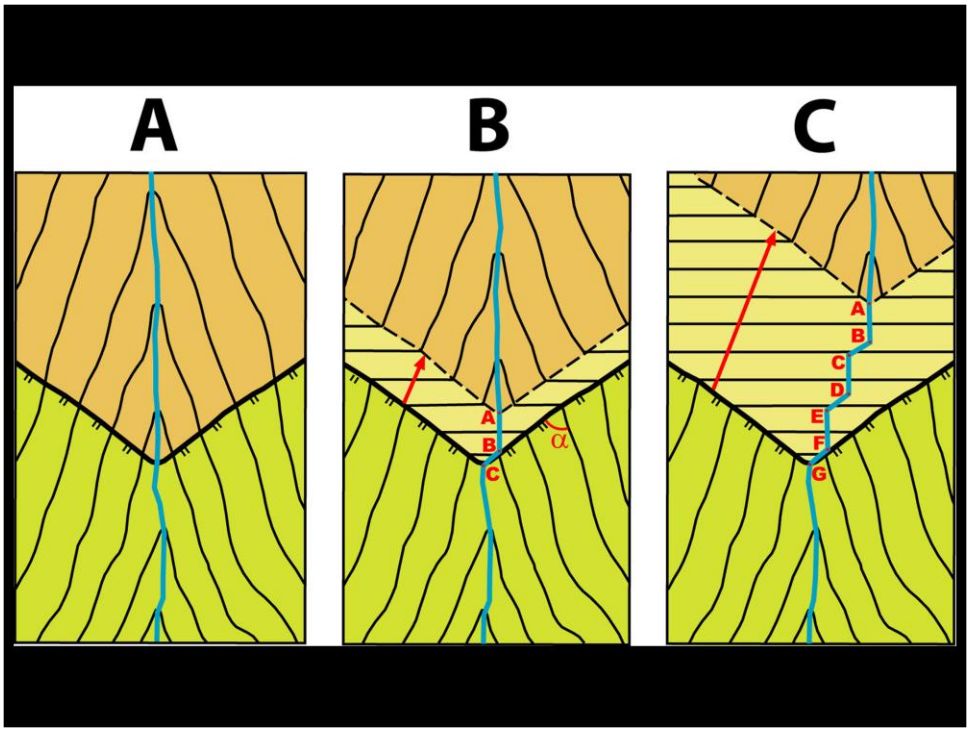

Contour map of topography associated with normal-fault slip that produces a planar fault ramp in the path of a stream. As long as angle alpha is less than 90 degrees, the stream will flow along the fault to re-enter the canyon segment in the hanging wall block. Frame B shows situation after one slip event, frame C after three. Arrow shows displacement of footwall relative to hanging wall. The ultimate result of multiple slip events is a displacement-parallel stream that is oblique to the down-slope direction on the fault ramp (from Spencer, 2000).

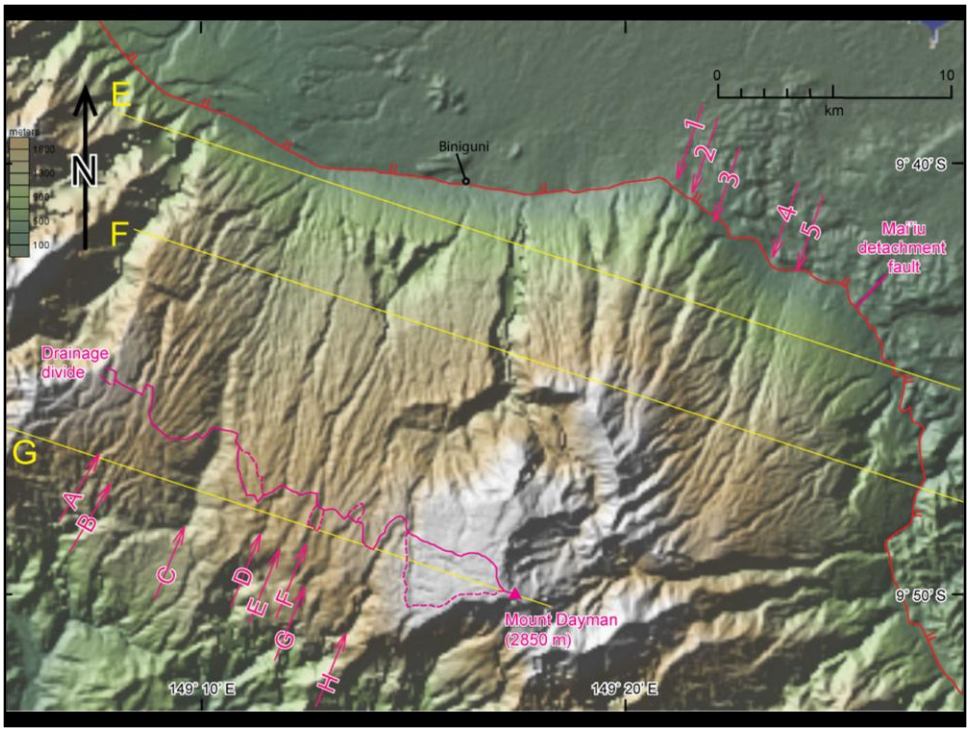

Dayman Dome metamorphic core complex in eastern Papua New Guinea, showing location of cross sections. Modified from Spencer and Ohara (2008). Topography derived from the Shuttle Radar Topography Mission digital elevation model, rendered using GeoMapApp.

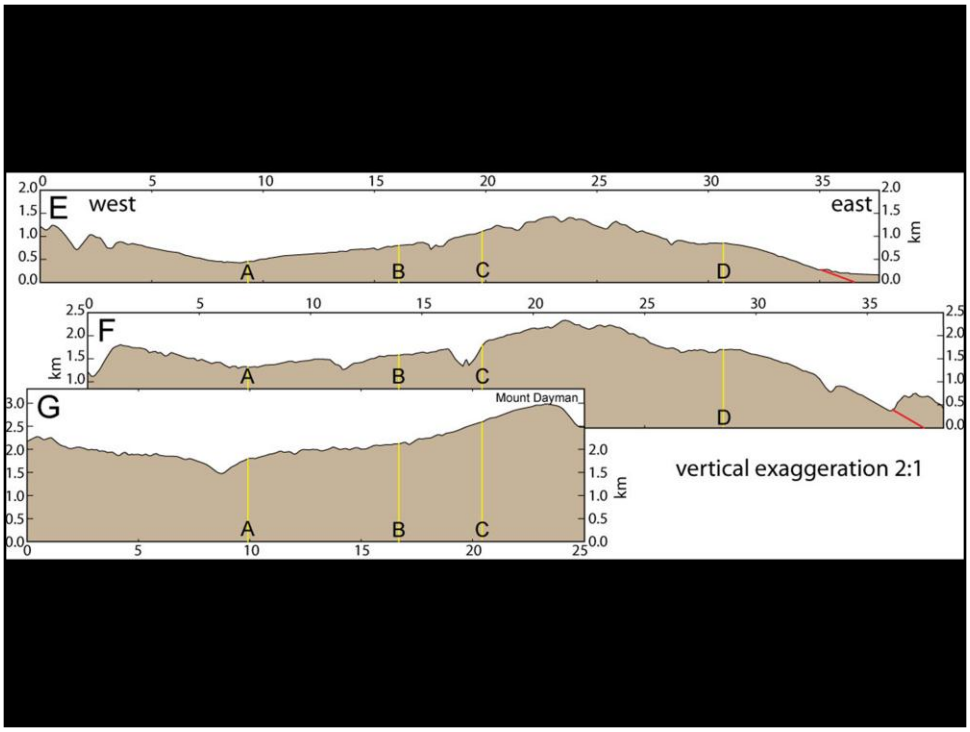

Cross sections of Dayman Dome metamorphic core complex in eastern Papua New Guinea. From Spencer and Ohara (2008). Topography derived from the Shuttle Radar Topography Mission digital elevation model, rendered using cross section tool in GeoMapApp.

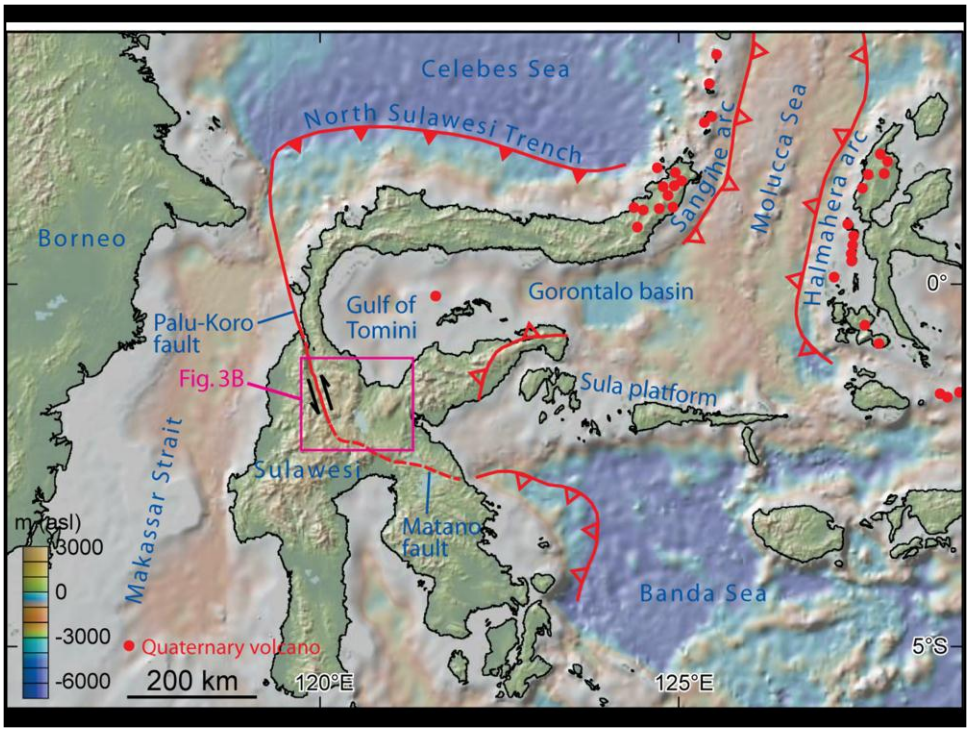

Sulawesi in central Indonesia. From Spencer and Ohara (2008). Topography derived from the Shuttle Radar Topography Mission digital elevation model, rendered using GeoMapApp.

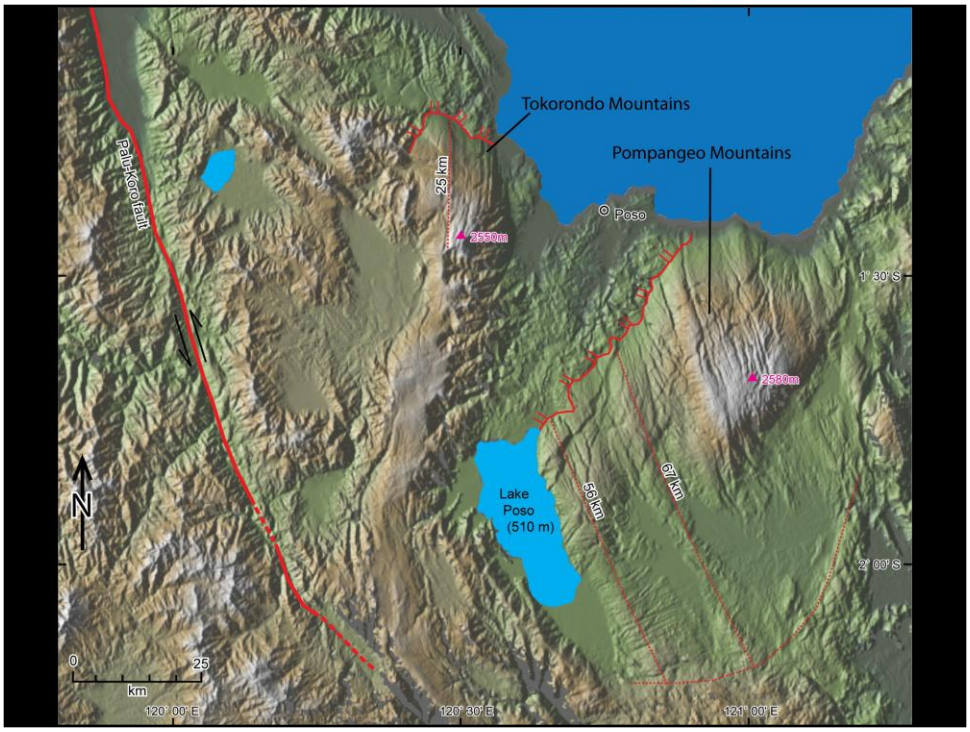

Central Sulawesi in Indonesia, showing locations of Pompangeo and Tokorondo core complexes, as interpreted by Spencer and Ohara (2008). From Spencer and Ohara (2008). Topography derived from the Shuttle Radar Topography Mission digital elevation model, rendered using GeoMapApp.

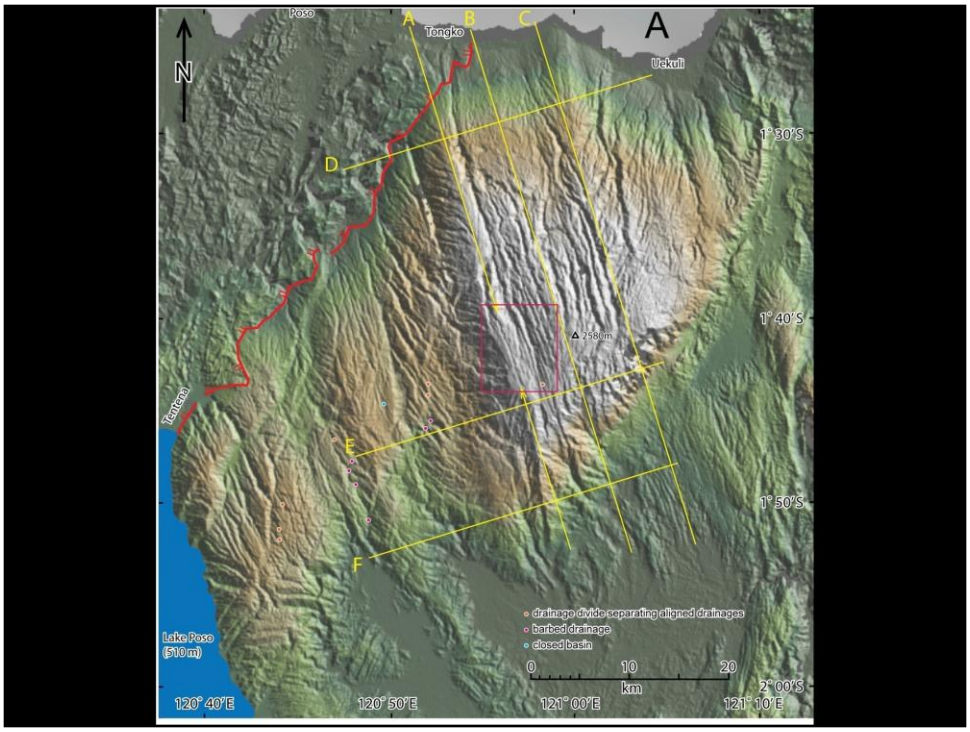

Pompangeo core complex as interpreted by Spencer and Ohara (2008), showing locations of cross sections and of aerial photograph presented by Hamilton (1979, figure 86). Topography derived from the Shuttle Radar Topography Mission digital elevation model, rendered using GeoMapApp.

Hamilton, W., 1979, Tectonics of the Indonesia region: U.S. Geological Survey Professional Paper 1078, 345 p., *with* Tectonic map of Indonesia, scale 1:5,000,000.

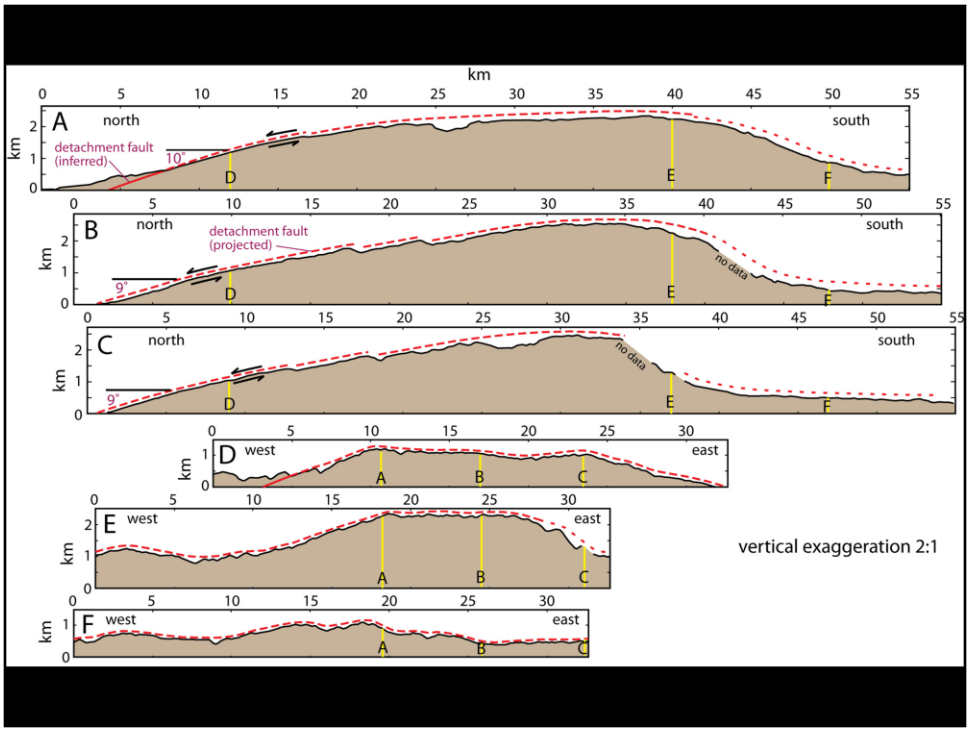

Topographic cross sections of Pompangeo core complex, central Sulawesi (from Spencer and Ohara, 2008). Topography derived from the Shuttle Radar Topography Mission digital elevation model, rendered using cross section tool in GeoMapApp.

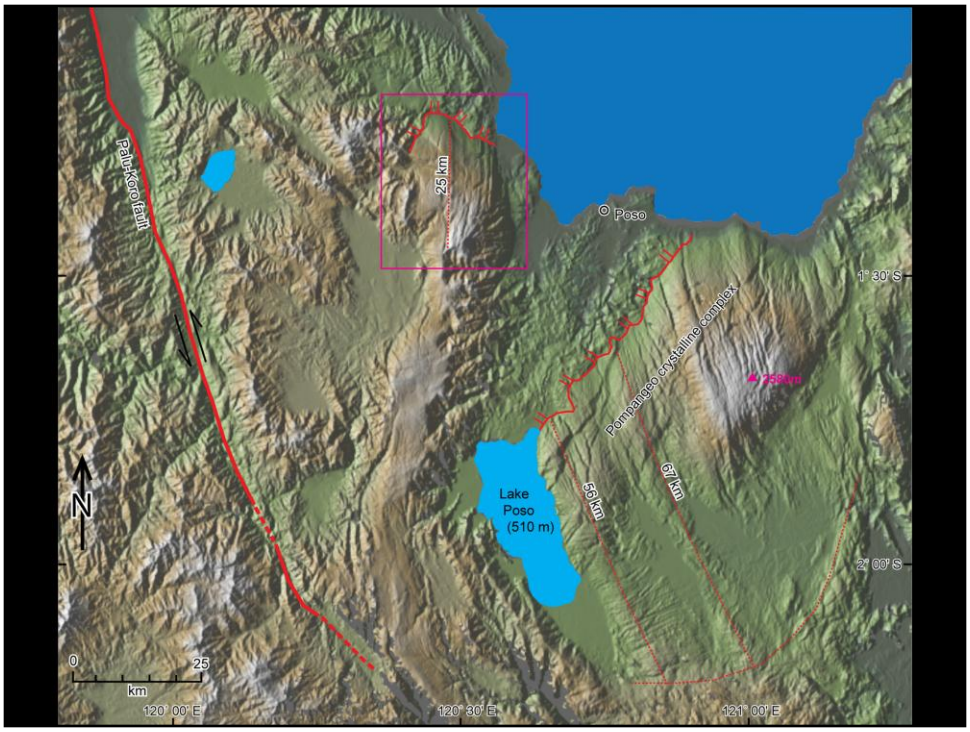

Central Sulawesi in Indonesia, showing location of Tokorondo core complex, as interpreted by Spencer (in review, 2009). From Spencer and Ohara (2008).

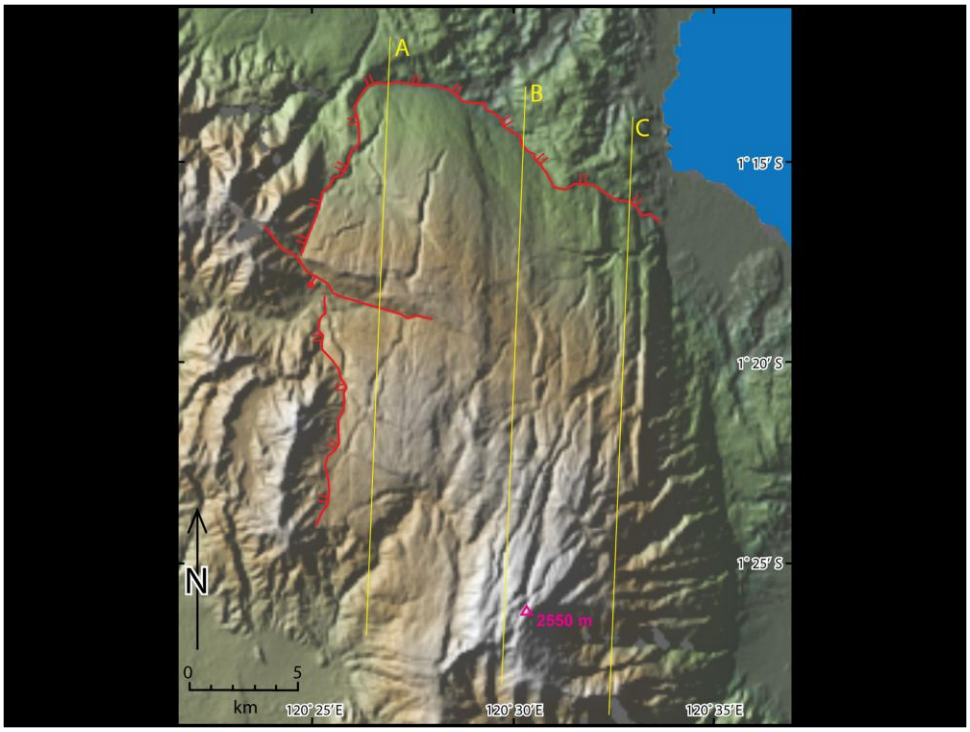

Tokorondo core complex, central Sulawesi, as interpreted by Spencer (in review, 2009). Topography derived from the Shuttle Radar Topography Mission digital elevation model, rendered using GeoMapApp.

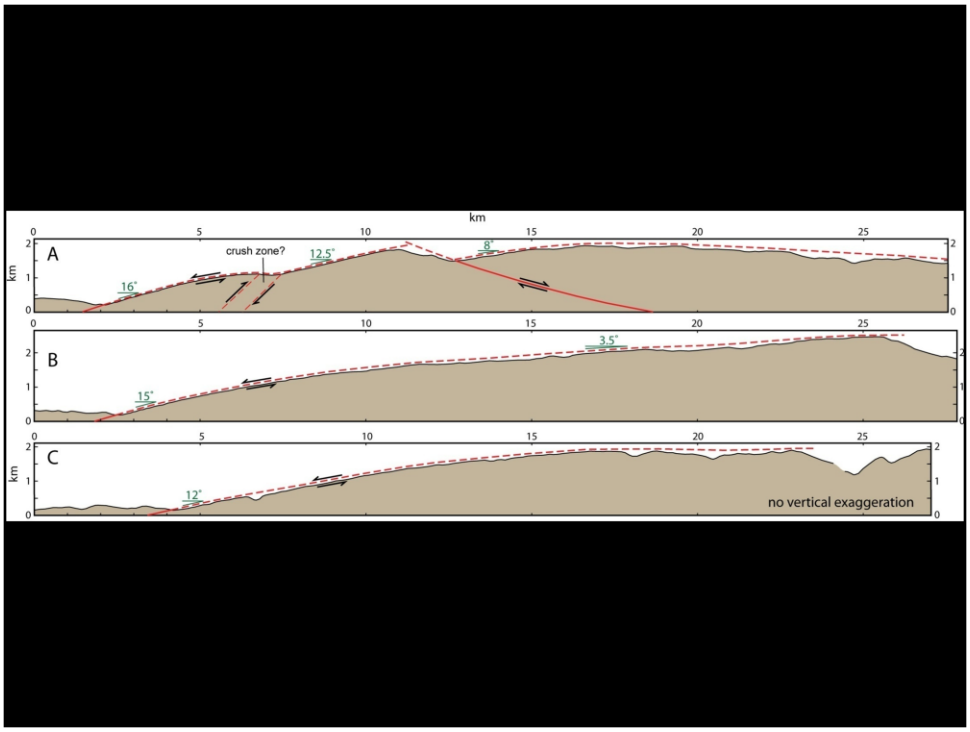

Cross sections through the Tokorondo core complex, central Sulawesi, as interpreted by Spencer (in review, 2009). Topography derived from the Shuttle Radar Topography Mission digital elevation model, rendered using cross section tool in GeoMapApp.

Venus, as revealed by synthetic aperture radar from the Magellan space probe.

Venus, as revealed by synthetic aperture radar from the Magellan space probe. From Spencer (2001).

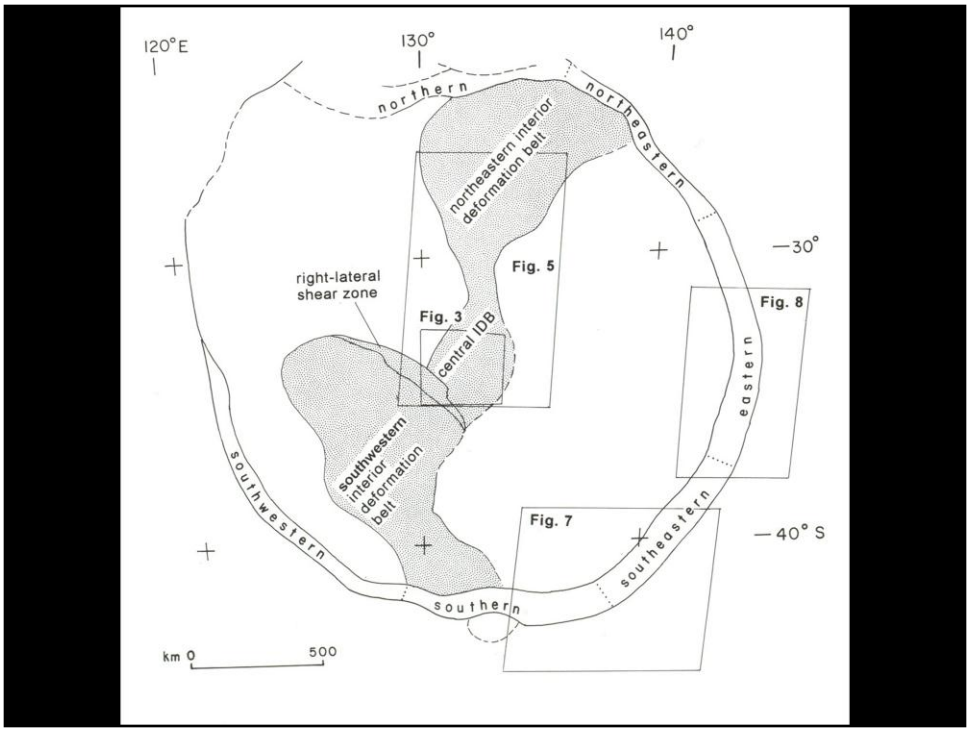

Map of Artemis Corona. From Spencer (2001).

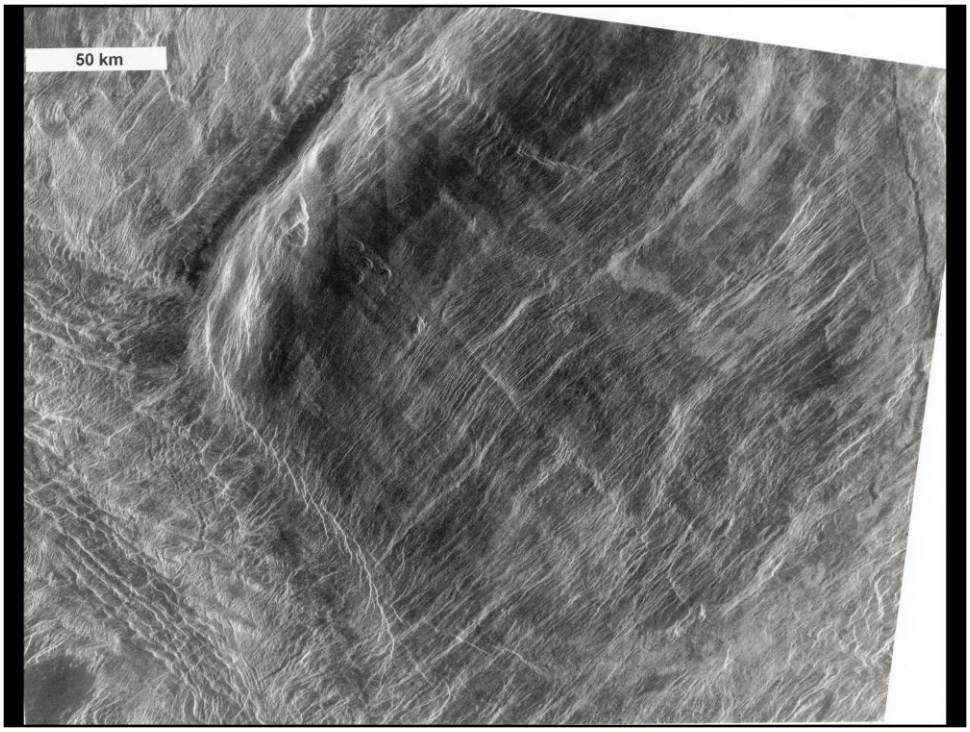

Central Artemis Corona, as revealed by synthetic aperture radar from the Magellan space probe.
Spencer (2001) interpreted this feature as a giant metamorphic core complex.

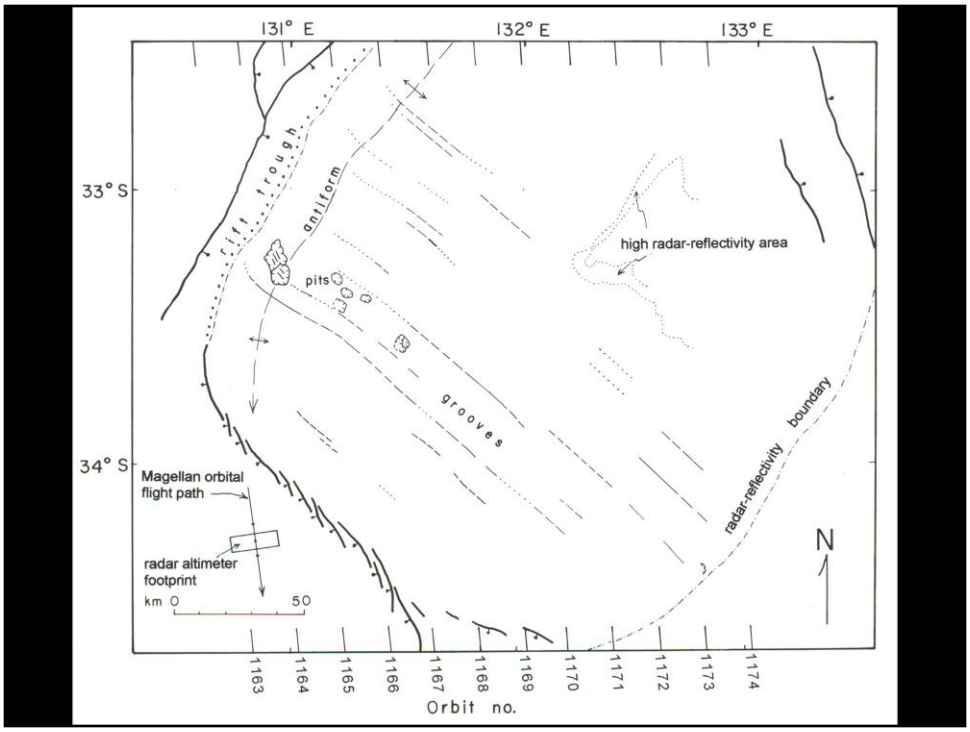

Central Artemis Corona, as interpreted by Spencer (2001) from synthetic aperture radar from the Magellan space probe. Grooves identified here are the longest known in the solar system.

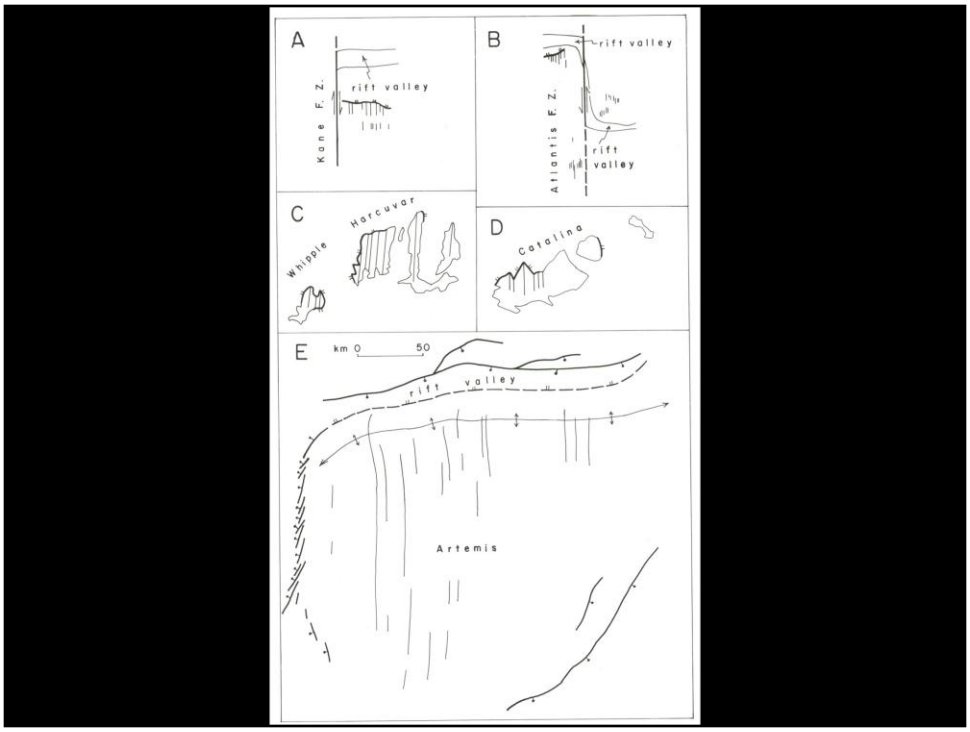

Comparison of core complex size. From Spencer (2001).

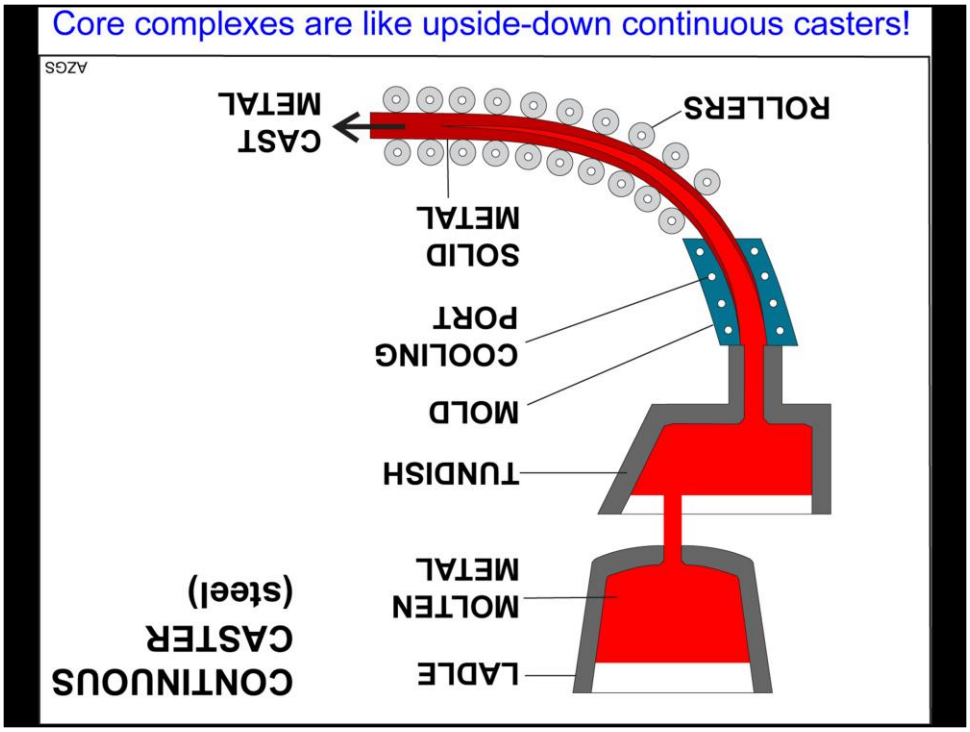

Core complexes are extruded with a geometry like and upside-down continuous caster.